JOURNAL OF AGRICULTURAL AND FOOD CHEMISTRY

Flavor Encapsulation in Yeasts: Limonene Used as a Model System for Characterization of the Release Mechanism

VALERY NORMAND,* GREGORY DARDELLE, PIERRE-ETIENNE BOUQUERAND, LAETITIA NICOLAS, AND DAVID J. JOHNSTON

Firmenich S.A., 7, rue de la Bergère, CH-1217 Meyrin 2 Genève, Switzerland

Empty yeast cells are used as a new delivery system for flavor encapsulation. The flavor release mechanism from yeast cells is characterized using a series of analytical techniques, and limonene is used as a model representing a hydrophobic flavor. Furthermore, the thermal stability of the capsules was assessed. The characterization of the cell wall structure gives rise to the development of an empirical model explaining water adsorption as well as the desorption singularities observed on drying. The study of the rate of flavor release as a function of temperature and water uptake in the cell wall clearly demonstrated a particular behavior of the yeast cell wall permeability. Below a water activity around 0.7, no flavor release is permitted whereas release occurs above it. Surface analysis on dry or wet cells using atomic force microscopy is discussed.

KEYWORDS: Limonene; *Saccharomyces cerevisiae*; sorption isotherm; temperature resistance

INTRODUCTION

As flavors are composed of volatile molecules, they are subject to large losses especially during the harsh processes of the food industry. A nonexhaustive list of food products, for example, coated fried food or in dough in fried noodles, often involves a high temperature treatment, conducive with flavor loss.

A method for minimizing flavor loss during such industrial processes is to confine the volatile molecules within a thermostable particle. One solution to this problem is to encapsulate the flavor molecules in an empty yeast cell (*1*).

The release mechanism of active material from delivery systems is of large interest for food, perfumery, and pharmacology industries. Understanding the release mechanisms allows a determination for safe storage conditions and identification of the optimal performance. Furthermore, determination of the optimal point of introduction of the flavor encapsulate within the food process can be identified.

The patent literature is generous regarding encapsulation of active material in yeasts (i.e., *2* and *3*). However, there is a need to enhance the understanding of the use of yeast cells as a delivery system and above all to elucidate the release mechanism.

De Nobel et al. showed that *Saccharomyces cerevisiae* could be used as a microencapsulation system (*4*). Nelson and Crothers (*5*) argued on the release mechanism and pointed out the role of water on the swelling and disruption of the cell wall and further speculated toward the reversibility of this process.

The aim of this study is to provide an understanding of the release mechanisms of flavor encapsulated in empty yeasts regarding different triggers, temperature under dry conditions, and relative humidity (RH) under conventional storage temperature conditions.

MATERIALS AND METHODS

Material. *S. cerevisiae* yeast provided by Firmenich SA (Item number 954794) was used in this work. Live yeast cells were pretreated with a plasmolyser in appropriate experimental conditions to remove most of the cytoplasmic material that occupies the cells (*6*). After several washing cycles with clear water and centrifugation, the empty yeasts were spray dried (*7*). Samples were used as such for unflavored yeasts or charged with a single hydrophobic molecule (limonene) using the procedure described in ref *2*.

Transmission Electron Microscopy (TEM). Samples for TEM measurements were prepared in three steps. Yeasts were immersed in 1% w/w osmium tetroxide solution for 2 h. The fixed samples were then washed in distilled water, enrobed in agar, and stained in uranyl acetate overnight. Subsequently, they were progressively dehydrated using aqueous ethanol solutions of increasing concentration (30 min in 70, 90, and 100% solutions) and finally acetone. Samples were put in acetone:resin (50:50 mixture) for 24 h and pure resin for 24 h before being embedded in TAAB resin (Hard plus, TAAB laboratories, Reading, United Kingdom) and polymerized at 55 °C in an oven for 48 h. Sectioning was performed using an Ultracut E microtome, and sections were stained using lead citrate before recording using a JEOL 1220 transmission electron microscope.

Thermogravimetric Analysis (TGA). TGA was performed on a TGA/SDTA 851e Mettler Toledo GmbH (Schwerzenbach, Switzerland). A mass of approximately 10 mg of sample was poured into an aluminum oxide crucible at 25 °C, and the sample was heated to 400 °C at 20 °C/min. The mass was recorded every 3 s and analyzed.

Differential Scanning Calorimetry (DSC). DSC was performed on a DSC 822e Mettler Toledo GmbH. Ten milligrams of sample was poured into an aluminum capsule at 25 °C and measured against air.

* To whom correspondence should be addressed. Tel: +41 22 780 21 91. Fax: +41 22 780 27 35. E-mail: Valery.normand@firmenich.com.

10.1021/jf0507893 CCC: $30.25
Published on Web 08/19/2005

The heating procedure was identical to the one used for the thermogravimetric experiment.

Phase Transition Analysis (PTA). Dry unflavored yeast samples were mixed with various amounts of water and homogenized using a high-speed mixer (Schweizer, Lausanne, Switzerland). The mixer ensured a homogeneous distribution of the water in the sample.

Two grams of yeast sample was introduced into the phase transition analyzer compression chamber (PTA 240, Wenger, Sabetha, KS) for determination of the powder's collapse temperature. The phase transition analyzer consists of a sealed chamber that is subjected to both a constant pressure and a linear increase in temperature. The piston displacement measures the compaction of the powder. Initial conditions were as follows: the pressure was preset to 120 bar for 15 s at 20 °C and then reduced to 100 bar for the time of the experiment. The temperature range was from 20 to 140 °C, and the temperature heating rate was 5 °C/min. The resulting displacement was fitted with a simple sigmoidal curve, and the collapse temperature was determined as the temperature for which the inflection of the sigmoid occurs.

Dynamic Vapor Sorption (DVS). The principle of the DVS system is to record the weight changes of a sample exposed to various RHs at isothermal conditions. Weight increase corresponds to water uptake, which will stabilize when the product reaches the equilibrium. DVS from Surface Measurement Systems (London, United Kingdom) was used in this study. A mass of approximately 10 mg was deposited on the microbalance plate. The initial RH was 40%, and the sample was left for 2 h prior to changing the RH. The temperature of the atmosphere surrounding the sample and the microbalance was accurately controlled. The measurement temperatures were 20 (70, 80, 85, and 90% RH), 30 (70, 80, 85, and 90% RH), and 40 °C (60, 70, 75, and 80% RH).

Drying experiments were conducted at 20, 30, and 40 °C. The sample was left at 40% RH for 2 h for equilibration. Then, the similar protocol as previously used was imposed in the reverse order, starting at high RH.

Atomic Force Microscopy (AFM). AFM was performed on a Nanoscope IV (Digital Instruments, Veeco group, Santa Barbara, CA), in the tapping mode in air and at ambient temperature. Dry yeasts (around 2 μm diameter) were spread on a mica slide. A similar procedure was carried out for yeasts mixed with a large amount of water left for 2 h at room temperature to allow removal of the excess water from the surface. The height imaging was achieved by using silicon nitride tips with a resonance frequency of about 250 kHz.

RESULTS

Morphological Characterization of the Yeast. *Microscopy of the Yeast.* The characterization of yeasts before and after loading was performed using TEM imaging. Images are shown in **Figure 1a**,**b** for empty yeasts and limonene-loaded yeasts, respectively. In TEM images shown in this paper, the dark material represents the undigested part of the cytoplasm while the gray material is characteristic of a lipid phase.

For unflavored yeasts, the proportion of empty cells as compared to filled cells is very high, thus demonstrating the efficiency of plasmolysis. The shape of the cells is spherical with a diameter slightly higher than 2 μm. A gray shell of around a few nanometers thickness delimits the cells. For loaded yeasts, a single large droplet of flavor (lipid) occupies most of the internal volume of the yeast.

Microscopy of the Yeast Cell Wall. The cell wall of *S. cerevisiae* consists of $\beta(1\rightarrow3)$glucans, mannoproteins, and a small amount of chitin. A structural model, combining proteins linked by disulfide bridges and glucan and mannan units, in equivalent amounts, linked by phosphates in a bed shape, was described (*8*). It is understood that $\beta(1\rightarrow3)$glucans maintain the rigidity (*9*) and mannoproteins maintain the porosity of the cell wall (*10*). In other words, mannoproteins are a filler for the skeleton of the $\beta(1\rightarrow3)$glucan network. The drying process used in the preparation of the yeasts forces water to evacuate the entire cell volume resulting in the shrinkage of the cell walls.

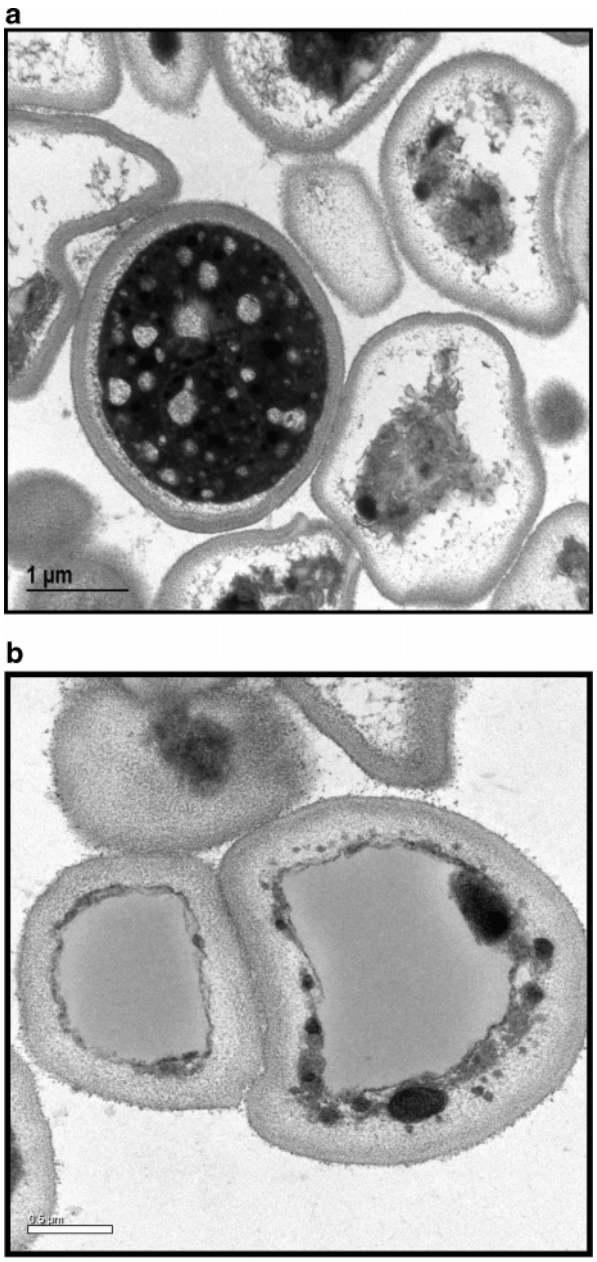

Figure 1. (**a**) TEM image of unflavored yeasts. (**b**) TEM image of flavored yeasts.

The typical protein content of dead cells is 30% in weight of dry matter whereas the polysaccharide fraction is around 50%.

A structural model proposed by Zlotnik et al. (*11*) places the major mannoproteins both at the surface and in deeper layers of the wall, shielding the cell wall $\beta(1\rightarrow3)$glucan from external enzymatic attack. **Figure 2** shows detailed TEM images of the dead yeast cell in similar preparation conditions for observation than in Zlotnik et al. (*11*). The preparation process (by proteolysis) of the yeasts does not affect the structure of the wall to a large extent, and two layers are still clearly distinguishable.

Similar to living cells, the structure of dead cells is composed of a thin protein layer that sits on a $\beta(1\rightarrow3)$glucan layer. The external protein layer is 15 ± 2 nm thick whereas the inner $\beta(1\rightarrow3)$glucan layer is 130 ± 17 nm thick. According to the average diameter of the dry cells (2 μm), the protein phase occupies around 10% of the volume of the cell wall as compared

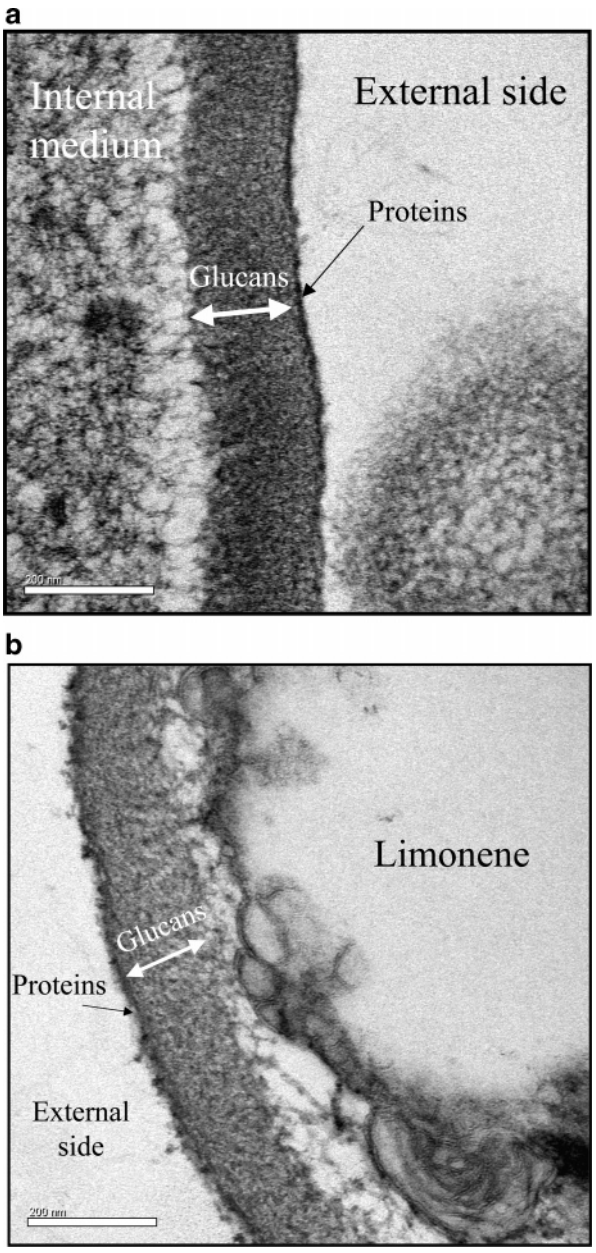

Figure 2. TEM detailed images of the structure of the cell wall for (**a**) unflavored and (**b**) limonene-flavored yeast. The scale bar is 200 nm.

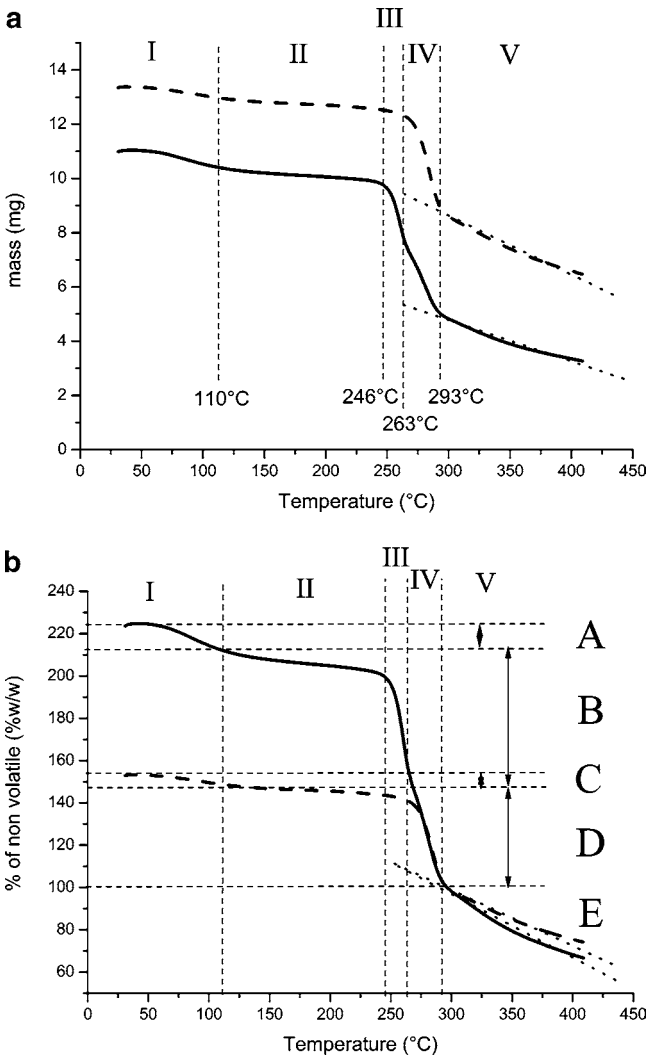

Figure 3. (**a**) Mass loss during heating (raw TGA data) for unflavored (dashed line) and flavored (continuous line) yeasts. (**b**) Normalized data for unflavored (dashed line) and flavored (continuous line) yeasts by the mass of dry material at 293 °C. A is for water in flavored yeasts, B is the flavor load, C is for water in unflavored yeasts, D is for volatiles inherent to the cells, and E is the nonvolatile components of the cells.

to 31% in living cells (*11*), and the polysaccharide phase occupies the remaining 90% as compared to 69% in living cells (*11*).

Thermal Stability. *Yeast Resistance to Temperature and Determination of Flavor Load.* The thermal stability in controlled dry nitrogen atmosphere condition is assessed using thermogravimetry. The temperature is increased gradually from 25 to 400 °C at 20 °C/min while recording the mass of the sample. Typical thermograms for empty and loaded yeasts are shown in **Figure 3a**.

The following phases are distinguished, being slightly different whether yeast is loaded or not. Domain I: This first temperature domain goes from 25 °C to around 110 °C. In this region, a slight mass loss is measured for both empty and loaded samples. As losses stop at 110 °C, we speculate that this is due to water evaporation. Furthermore, this is closely correlated with an independent measurement of water content. The Karl Fischer water determination method gives 3.8 ± 0.2% w/w and 3.3 ± 0.3% w/w for empty and loaded yeasts, respectively, whereas TGA gives 4.1 and 3.4% w/w for empty and loaded yeasts, respectively. It is speculated that water is only present in the cell external shell, thus making it readily available.

Domain II goes from 110 to 246 °C. Here, the mass remains approximately constant. In this phase, the cells are free of water and only heating of organic material occurs (yeast material with or without flavor).

Domain III: The difference between empty and loaded yeasts is shown in this domain. For loaded yeasts, domain II ends up at a lower temperature (246 °C) where domain III starts. This domain, which goes from 246 to 263 °C, is only observed for loaded particles. The important loss observed is interpreted as such: evaporation of limonene either by forced diffusion of the gaseous limonene through a porous cell wall (partial disruption of the shell) or by mechanical rupture of the cell wall generated by the increasing inner pressure. For empty particles, domain II ends up at 263 °C when domain IV starts.

Domain IV, which shows superposition for empty and loaded yeast, goes from 263 to 293 °C. A huge mass loss is measured. At this stage, it is supposed that the cell wall rupture occurs, allowing the liberation of the gaseous compounds inherent to the yeast.

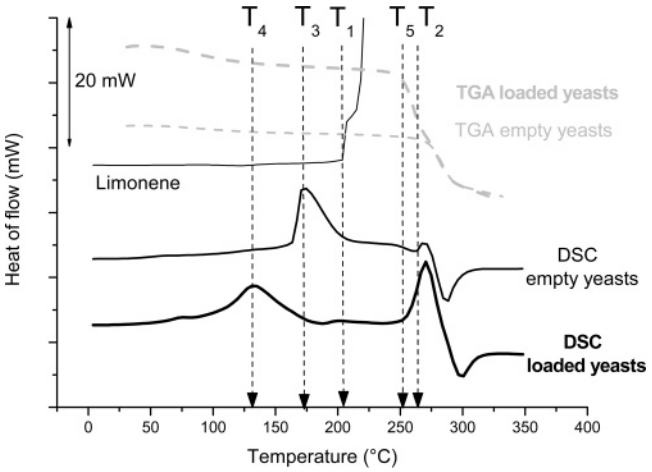

Figure 4. Calorimetric traces of three samples (TGA measurements of **Figure 3b** are superimposed). The legend is on the graph. The critical temperatures for events are signaled on the graph and explained in the text.

Domain V goes from 293 to at least 400 °C. Here, the rate of loss is constant but lower than in domains III and IV. In domain V, the dry constituents of the cells are unstable, and at the end of the experiment (400 °C), all samples are carbonized.

Normalized data by the amount of dry material (point at the boundary between domains IV and V) are presented in **Figure 3b**. The slopes in domain V are now superimposed for both loaded and unloaded yeasts. This indicates clearly that the material in domain V is identical and the normalization using the mass of dry material is coherent.

The difference (loaded − empty) of normalized data that corresponds to the loss observed in domain III was found to be 26.7% w/w of pure limonene. The limonene content was confirmed using NMR-low field measurements. However, the yield depends on the flavor molecules to be encapsulated (*1*).

Calorimetric Measurements and Localization of the Flavor Encapsulated. A DSC experiment was conducted to observe the temperatures at which energy is needed and to localize the different events seen according to the TGA measurements. Three samples are compared in **Figure 4**: limonene alone, empty yeasts, and yeasts containing 26.7% w/w of limonene.

The temperature of vaporization of pure limonene is $T_1 = 204$ °C under the experimental conditions used. Empty yeasts (light line in **Figure 4**) present an endothermal peak at $T_3 = 173$ °C that is shifted toward lower temperatures ($T_4 = 131$ °C) when limonene is encapsulated in yeasts, without any significant loss of weight (see **Figure 3**). This peak is interpreted as a melting temperature of a crystalline region; probably hydrophobic interactions within the phospholipid membrane. Consequently, the shift of this melting peak when limonene is encapsulated indicates that limonene is located within the membrane, lowering the cohesive energy of the phospholipidic bilayer. A signal interpreted as a vaporization or destruction of the shell (interpretation of the TGA) is located at $T_2 = 263$ °C for empty yeasts, and for limonene loaded yeasts, the flavor molecules evaporate at $T_5 = 251$ °C, which corresponds to the temperature at which the loss of mass increases strongly (see **Figure 3**).

At 246 °C, calorimetric results (**Figure 4**) show that limonene evaporates. This confirms gravimetric results (**Figure 3a**). Therefore, it is suggested that the cell wall that is still stable until 263 °C, independently of the flavor content, becomes permeable to gaseous flavor molecules, or it cannot sustain the inner pressure and breaks. The structural model and the release due to thermal stress are summarized schematically in **Figure 5a**,**b**, respectively.

Effect of Water on the Yeast Cell Wall Properties. *Empty Cells: Sorption and Desorption Isotherms.* The water weight fraction (corrected by the initial water content measured by the Karl Fischer method) is determined from the DVS experiments on unflavored sample using eq 1.

$$X_W = \frac{m_0(X_{W0} - 1) + m_{tot}}{m_{tot}} \quad (1)$$

In eq 1, X_W is the total weight fraction of water, m_0 is the initial mass of the sample before the experiment starts, X_{W0} is the initial water weight fraction measured by the Karl Fischer method or by TGA, and m_{tot} is the total weight of the sample.

X_W was determined for unflavored yeasts between 40 and 90% RH and at three temperatures: 20, 30, and 40 °C. A typical sorption/desorption experiment is presented in **Figure 6a**.

On sorption, an increase of the sample weight is observed when the RH increases. After 1 h, for each RH, the weight of the sample stabilized and equilibrium was reached (slope zero, the mass is stable). The maximum water uptake, obtained for 90% RH and 20 °C, is roughly 20% w/w under the conditions of measurement. On desorption, gradually, the water content decreases when the RH decreases. Similarly to the sorption kinetics, an apparent equilibrium is reached after 1 h at any given RH, but the water content is higher than the one obtained for sorption at the same RH. This is the hysteresis largely described in the literature for water sorption/desorption on biopolymer materials. The water concentration at each RH plateau is represented in **Figure 6b** and fitted using the Guggenheim−Anderson de Boer model [GAB model (*12*); see eq 2].

$$X_w = \frac{X_m C K a_w}{(1 - K a_w)(1 - K a_w + C K a_w)} \quad (2)$$

In eq 2, X_w (% w/w) is the equilibrium material moisture content, X_m (% w/w) is the monolayer material moisture content, C is the Guggenheim constant, K is the molecule multilayer factor, and a_w is the water activity that corresponds to the ratio of the partial pressure of water over the measurement pressure. Measurements have been carried out under atmospheric pressure conditions; therefore, a_w equals the RH in air. The experimental data for the three temperatures are well-fitted by the model.

When RH increases, there is no huge temperature effect for water uptake in the investigated temperature domain. A hysteresis is observed on decreasing the RH, but still, the data are well-fitted using the GAB model. This shows the semireversibility of the water uptake. The results concerning the three empirical fitting parameters of the GAB model are summarized in **Table 1** and discussed below.

For sorption isotherms, the monolayer material moisture content (X_m) is higher at 40 °C than at lower temperatures as demonstrated for model carbohydrate samples (*13*). However, the concentration X_m does not evolve much with the temperature and is close to the initial water content of the yeast. This indicates that the volume that takes water is limited (cell wall) and is subject to swelling limited by the reticulation of the biopolymers.

Loaded Yeasts: Rate of Flavor Evaporation. In 1974, Scherrer et al. (*14*) stated that only molecules smaller than 700 g mol^{-1} are allowed to diffuse freely through the cell wall of

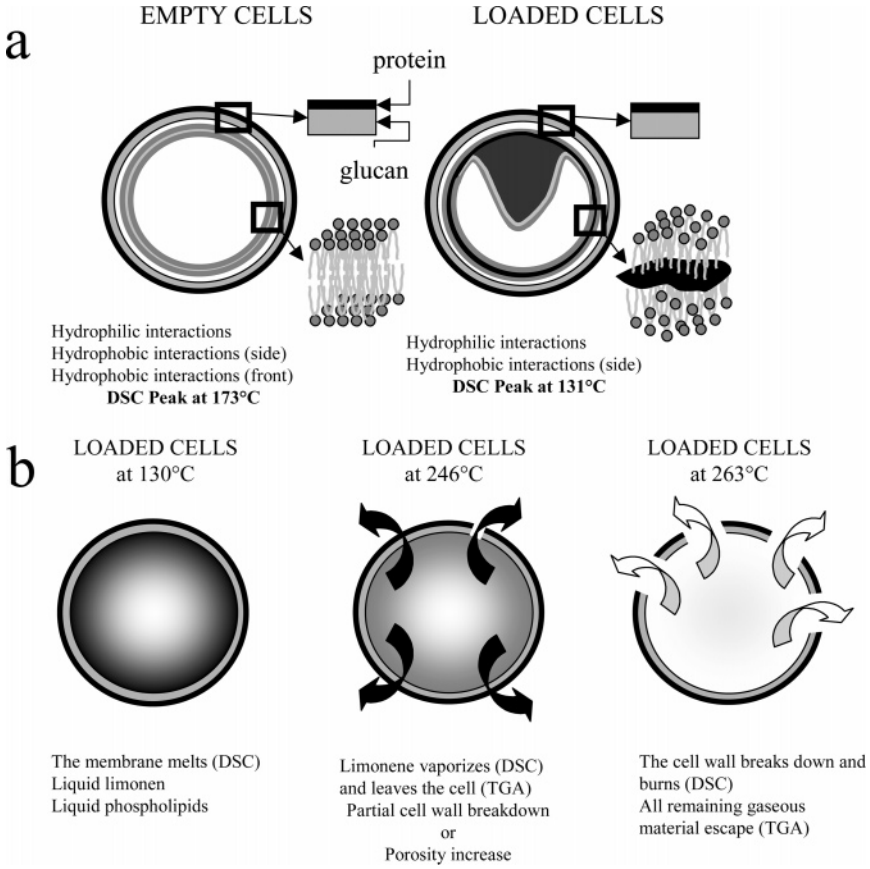

Figure 5. Schematic representation of (**a**) the structure of the empty and loaded yeast and (**b**) the temperature stability of the loaded yeasts.

living yeasts. However, since then, this limit has been demonstrated to be much larger for globular proteins (as long as 400000 g mol^{-1}) (*15*).

With the samples containing limonene (Mw = 136 g mol^{-1}), an identical DVS experiment has been conducted on dry yeasts from 40 to 90% RH at 20, 30, and 40 °C. Raw data at 40 °C of the evolution of the mass over time for various RH conditions are shown in **Figure 7**. The composition of the flavored sample was assessed by thermogravimetry, and the water and limonene contents were 5.1 and 26.7% w/w, respectively.

It is shown here that for RH below 60% the yeast reaches equilibrium as if it was empty. However, for RH over 60%, the equilibrium is never reached as a linear loss of weight is observed with time. The higher the RH is, the higher the rate at which the sample loses weight. This is attributed to a zero-order kinetic loss of limonene.

Deformability Properties. The PTA has recently been proven to be a reliable technique to measure the glass transition of maltodextrin powders (*16*). Empty yeasts mixed with various amounts of water were tested in the PTA chamber. The evolution of the compression is revealed by the displacement of the piston. Results are shown in **Figure 8** for water mass fractions ranging from 3.8 to 20% w/w.

In **Figure 8**, it is shown that water affects the compaction of the yeast pile under pressure. We define empirically an apparent transition temperature (or collapse temperature) for the yeast cells as the temperature at which the sample collapses. We consider this temperature as the temperature at which the inflection of a sigmoidal fit of the displacement against temperature occurs. Collapse temperature values are reported in **Figure 8** for 3.8, 4.8, and 8.4% w/w water content and are 102.5, 74.1, and 63.4 °C, respectively. At 20% w/w water content, the yeast pile already collapsed at room temperature indicating that the collapse temperature might be much lower.

DISCUSSION

To demonstrate the water-induced mechanism of flavor release from loaded yeasts, the sorption and desorption isotherms on empty cells need to be understood. The presence of limonene inside the yeast should not interfere with water gain or loss if the cell wall is sensitive to water.

Empty Yeast Cells. *Modeling Sorption/Desorption Isotherms.* As suggested by Guggenheim−Anderson−deBoer, C and K parameters in eq 2 evolve with temperature according to Arrhenius (see eq 3a,b).

$$C = C_0 \exp\left(\frac{H_m - H_n}{RT}\right) = C_0 \exp\left(\frac{H_C}{T}\right) \quad (3a)$$

$$K = K_0 \exp\left(\frac{H_n - H_l}{RT}\right) = K_0 \exp\left(\frac{H_K}{T}\right) \quad (3b)$$

Here, H_m is the heat of sorption of a monomolecular layer of water, H_n is the heat of sorption of a multimolecular layer of water, H_l is the heat of condensation of water vapor, and H_C and H_K are two simplifying parameters expressed in Kelvin. The temperature dependence of these parameters is shown in **Figure 9**.

For desorption, X_m, K, and H_K {that is, the slope d[ln(K)]/d(T^{-1}), not represented in **Figure 9**} are not evolving much. However, the parameter C tends toward infinite values (see parameter values in parentheses in **Table 1**) and induces the hysteresis observed between the sorption and the desorption of water molecules. Kinetics arguments are usually reported, as

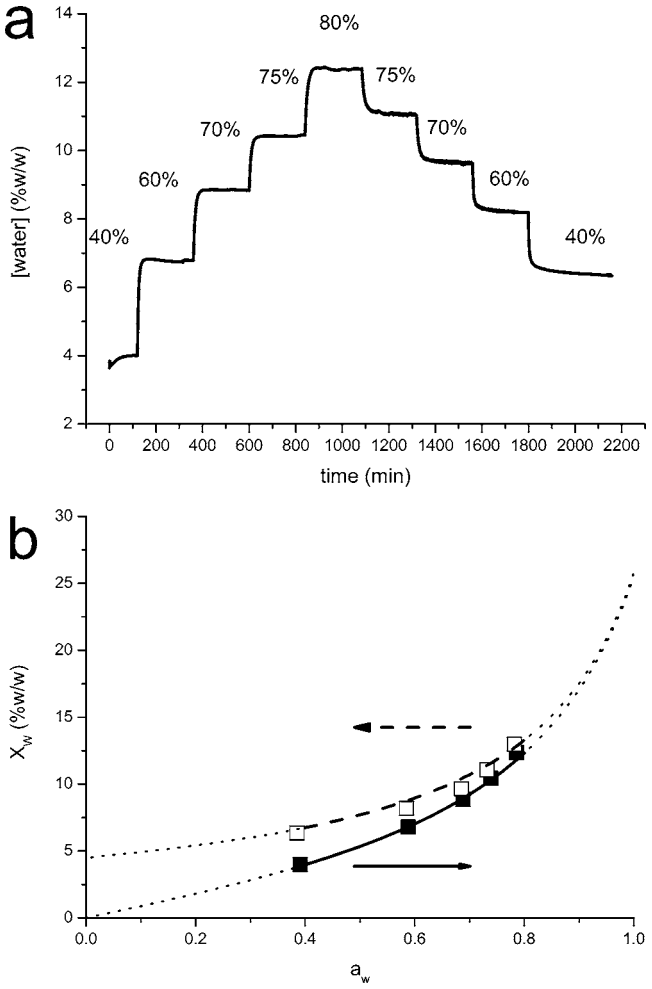

Figure 6. (**a**) Typical kinetics of yeast water content change during sorption and desorption experiments at 40 °C. (**b**) Water content of unflavored yeasts at 40 °C as a function of the water activity in the gas phase plain squares for increasing RH and empty squares for decreasing RH. The lines correspond to the best fit using the GAB model for sorption (plain) and desorption (dashed) isotherms.

Table 1. Parameters of the GAB Model for Three Temperatures[a]

temp (°C)	X_m	C	K
20	4.54 (5.12)	3.29 (∞)	0.872 (0.847)
30	5.11 (5.04)	2.48 (∞)	0.835 (0.827)
40	5.72 (4.52)	1.90 (∞)	0.801 (0.824)

[a] Fitting parameters for desorption are in parentheses.

the thermodynamic alone cannot explain such behavior, and time for equilibration during desorption is much greater than for sorption (*17*). Also, structural arguments have been suggested as the polymer may undergo relaxation by losing water that is energy demanding.

Nevertheless, a large discrepancy for C between the sorption and the desorption has already been reported for relatively low polymerization number average α-glucan oligosaccharides (*13*), and in our case, eq 2 simply reduces to eq 4:

$$X_w = \frac{X_m}{(1 - Ka_w)} \tag{4}$$

To understand why C becomes infinite for desorption, the following comment is necessary: There are similarities between

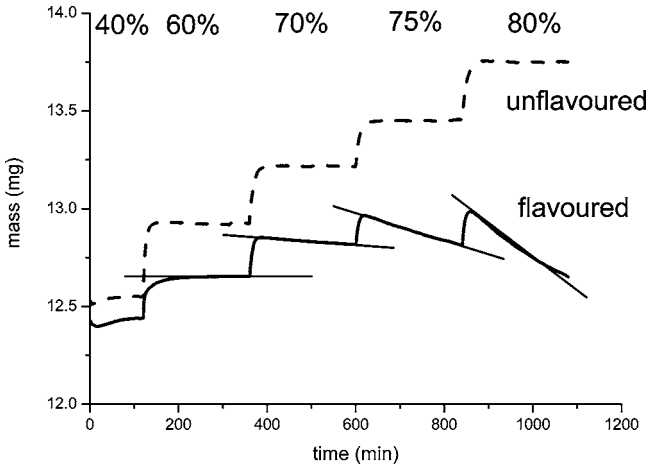

Figure 7. DVS experiment on unflavored (dashed) and flavored (plain) DHW yeasts at 40 °C and at various RH: 40% for 2 h, 60% for 4 h, 70% for 4 h, 75% for 4 h, and 80% for 4 h. The results represent the evolution of the mass of the sample (mg). The release of the flavor is linear with time.

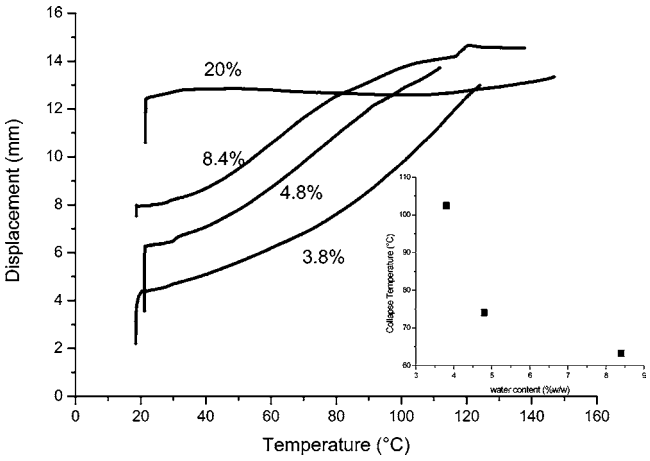

Figure 8. Displacement trace of the phase transition analyzer for unflavored yeast cells containing various amounts of water. The solid line represents the piston displacement.

the C parameter introduced in the Brunauer−Emmett−Teller (BET) equation (*10*) and the C parameter used in the GAB equation (*12*). The BET model considers only two water species or layers but has a clearer physical meaning than the GAB empirical model (*18*). In fact, one can see that C for the BET model evolves like the product $C{\cdot}K$ for the GAB model, with K always lower than unity. According to **Figure 9**, K varies far less than C when the temperature changes. Therefore, C in the GAB model is identical to a constant fraction of C in the BET model especially if C tends toward infinity.

C_0 in eq 3a, according to the BET multiple layer model, was defined as a function of rate constants for sorption and desorption of water molecules (*10*). The BET C constant writes as eq 5:

$$C_0 = \frac{a_1 b_2}{b_1 a_2} \tag{5}$$

In eq 5, the subscripts 1 and 2 represent the first and the second layers of adsorbed water molecules, respectively, and a and b are the kinetic constants for sorption and desorption of water molecules, respectively. a_2 and b_2 concern the water sorption and desorption on the second water layer, "far" from the material

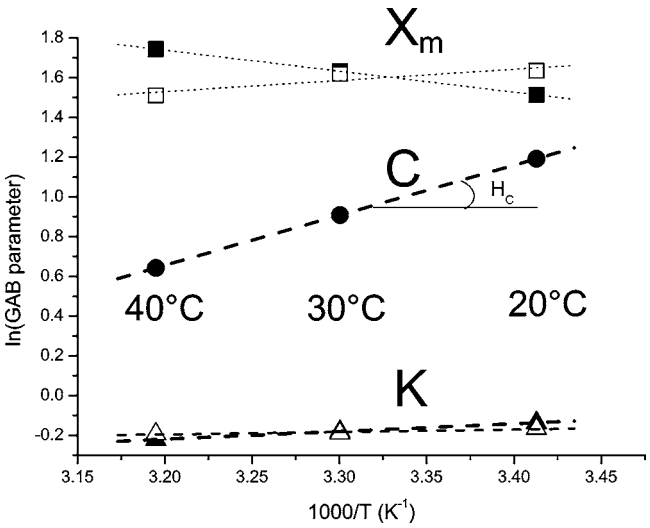

Figure 9. Arrhenius plot of the GAB parameters on sorption (solid scatters) and desorption (open scatters) for the three temperatures. For sorption, H_C (materialized) and H_K (that is not shown) are the slopes characterizing the evolution of ln*C* and ln*K* with the reciprocal temperature, respectively.

constituting the wall of the yeast. a_1 describes the water sorption from the air to the surface of the yeast. The only possibility for C_0 to converge toward an infinite value is when b_1 tends toward zero. b_1 is the rate constant for water desorption from the layer in contact with the surface of the polymer (deep water). b_1 equaling zero means that the water molecules solvating the polymer cannot leave the yeast or the polymer phase in the case of a pure single polymer. An interpretation of this result could be due to the composite structure of the yeast cell wall.

The hypothesis presented here is that for sorption, water molecules adsorbed by the external mannoprotein structures (*19*) can easily migrate deeper in the yeast cell wall, toward the structure formed by $\beta(1\rightarrow3)$glucan (see **Figure 2**). Thus, it is commonly found that polysaccharides dehydrate proteins in food systems (*17*). The driving force for water to reach a deeper zone of different chemical structure will then be governed by the nature and the molecular weight of the different supporting phases. It is important to note that at equilibrium, the water activity (a_w) is identical in all of the different coexisting phases whereas the water concentration (X_w) depends on the affinity for water of the individual phases (different sorption isotherms). For desorption isotherms or drying isotherms, the process is different. Water can reach the air phase only from the protein phase. It seems reasonable to consider (at a first approximation) that the rate for the air phase and the protein layer to reach equilibrium is very fast due to the reduced thickness of the protein layer (15 nm). However, the large amount of water adsorbed on the β-glucan deeper and thicker layer has to migrate through the protein layer in equilibrium with the air phase. This is necessary to reach equilibrium between the β-glucan and the protein layers. If the concentration of water in the protein phase is low, it decreases also its diffusion coefficient and therefore its rate of migration (*20*) [i.e., The evolution of the diffusion coefficient of water evolves exponentially with its phase volume fraction in a binary polymer/water mixture (*21*)]. The protein layer can also go through a second-order phase transition to become more compact; thus, the diffusion rate of water through the phase becomes close to zero.

This mechanism is the key to explain with kinetic arguments, the temporary cessation of life processes in yeasts (*22*), keeping the maximum water available inside the cell for the survival of vital functions. Complete drying of the cell is accessible experimentally by giving the system enough energy to extract the water molecules (*22*). This is done industrially using spray drying or experimentally using temperature (see **Figure 3**). The extent of the hysteresis observed for yeasts is then related to the kinetics of diffusion through biopolymer phases of various structures. A complete modeling of the water permeation in the cell wall would be possible once the components of the structure will be isolated and measured independently of one another, which is premature at the moment. However, an attempt to model the water sorption isotherm of a bilayer structure can be derived to infer the shape of the water sorption isotherm and validate the use of the GAB model in the present case.

The two-layer structure involves two equilibriums when water sorption and desorption are considered. The water content is different in the two layers, but the water activities are identical at equilibrium. A simple model based on additivity rules (eq 6) demonstrates that in the initial proportions of phases given above (phase volumes significantly different), the resulting water uptake can still be empirically and accurately approximated using the GAB model.

$$X_{WM} = \frac{\sum_i \frac{X_{mi} K_i C_i a_W}{(1 - K_i a_W)(1 - K_i a_W + K_i C_i a_W)} \phi_i}{\sum_i \phi_i} \quad (6)$$

In eq 6, the subscript "*i*" stands for the layer number that is supposed to be homogeneous and ϕ is its phase volume. As suggested, if ϕ_1 approaches one-tenth whereas ϕ_2 corresponds to the nine remaining tenths of the membrane volume, eq 6 can still be fitted using eq 2 where all parameters involve the contribution of each phase. Of course, this assumption is oversimplified but it helps the understanding of the experimental observations. Also, it has to be emphasized the fact that the GAB or the BET models are widely used for complex food systems disregarding the complexity of the structure or nature of the sample.

Let us first define one hypothetical isotherm of sorption for each phase that is well-described by the GAB model (*17*). The parameters of the GAB fit have to show that the polysaccharide phase takes more water than the protein phase at identical water activity (*17*) comprised between 0 and 0.8. It has been reported for a series of proteins and polysaccharides that the isotherms of sorption are steeper for proteins at large water activities (over 0.8) than those for polysaccharides [i.e., apple pectin vs sodium caseinate (*23*)]. In **Figure 11a**, the hypothetical GAB isotherms of water sorption for the individual layers are presented. For the protein phase, X_m, *K*, and *C* are 7.0, 0.91, and 0.4, respectively, and for the β-glucan phase, X_m, *K*, and *C* are 5.8, 0.80, and 3.0, respectively. The morphological wall characteristics of a model spherical yeast cell of 2 μm diameter are defined as follows according to **Figure 2**: The thickness of the protein layer is 15 nm, and the thickness of the $\beta(1\rightarrow3)$glucan layer is 130 nm. The densities are taken arbitrarily as 1.0, 1.3, and 1.6 g cm^{-3} for the water (d_W), the protein (d_P), and the $\beta(1\rightarrow3)$glucan ($d_{\beta-G}$), respectively. The cell wall volume increase due to the water uptake is calculated according to the individual layer water uptake and allows calculation of volumes fractions for each phase (ϕ) at any water activity. The total volume of the cell wall is the volume occupied by the two layers:

$$V_{CW} = V_P + V_{\beta-G} \quad (7)$$

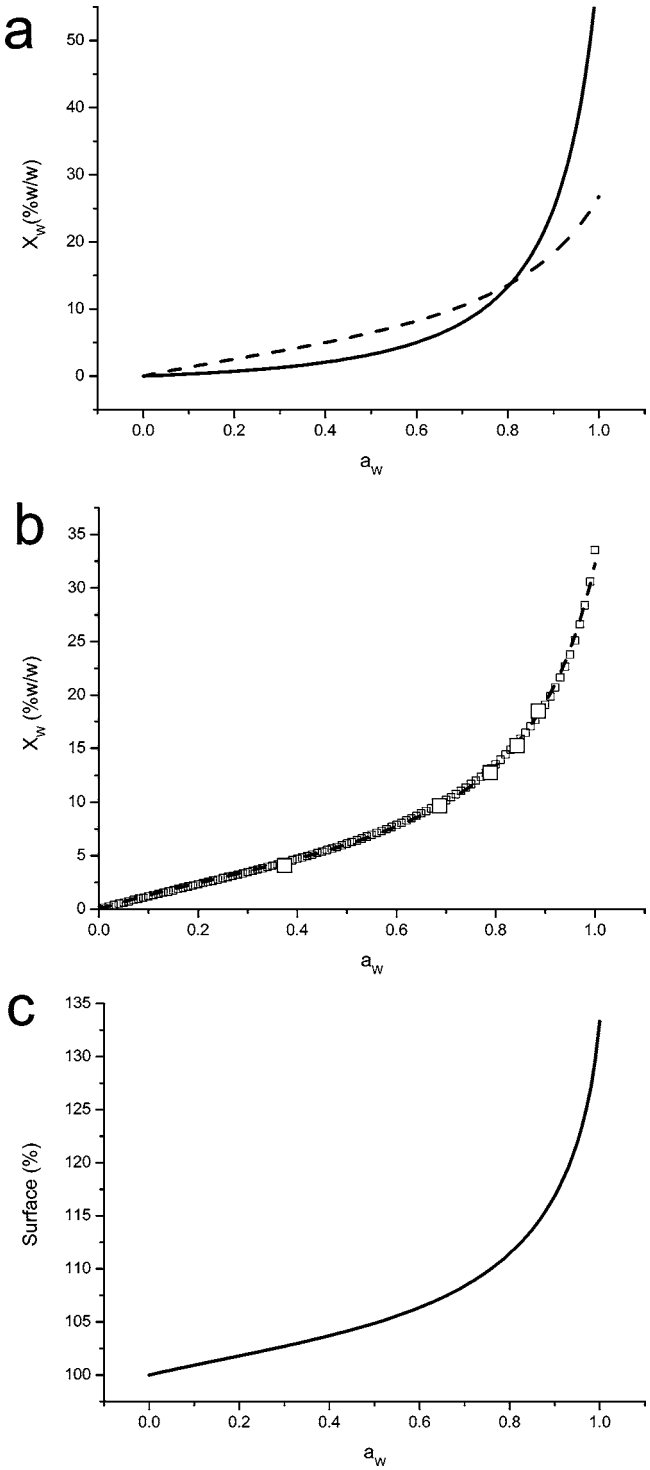

Figure 10. (**a**) Isotherms of sorption for individual phases; the line is for protein, and the dashed line is for β-glucan. (**b**) Isotherm of sorption for the composite structure of the cell wall as calculated using eq 10 (small squares) and fitted using eq 3 (dashed line). Experimental data points at 20 °C are the large open squares. (**c**) Evolution of the external yeast surface with the water activity relative to the initial surface of the cell.

The cell wall volume (V_{CW}), the volume occupied by the protein (V_P), and the volume occupied by the $\beta(1\rightarrow3)$glucan ($V_{\beta-G}$) are all functions of the water activity. The two volume fractions for the individual phases are calculated according to:

$$\phi_P = \frac{V_P}{V_{CW}} = 1 - \phi_{\beta-G} \tag{8}$$

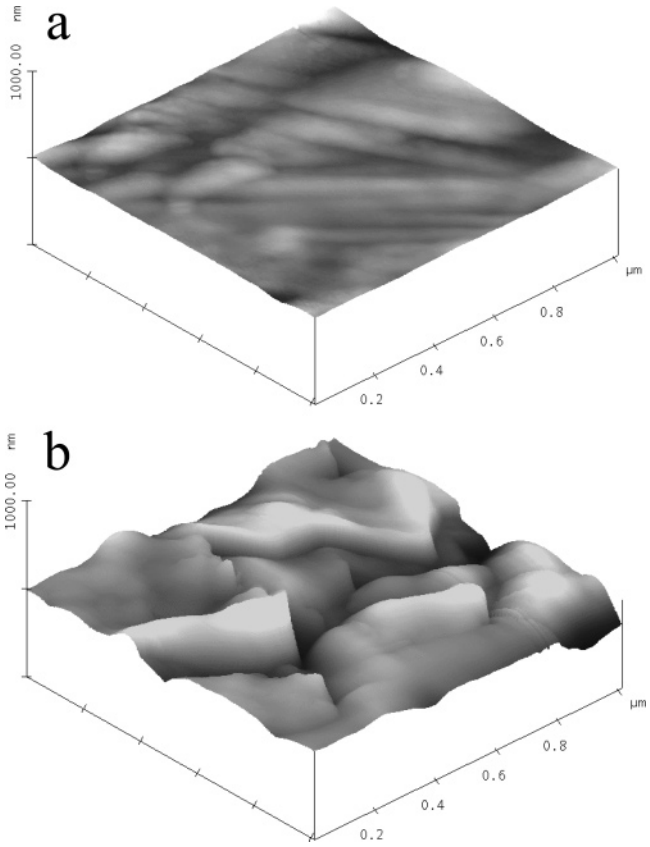

Figure 11. AFM micrograph of yeast cells surfaces (**a**) dry yeast (3.8% w/w water) and (**b**) wetted yeast (water content higher than 20% w/w).

Knowing the concentration of water taken at a given water activity (**Figure 10a**) and knowing the initial volume of the considered phase (V_{P0} and $V_{\beta-G0}$), the volume increase due to the water uptake is given by:

$$V_P(a_W) = V_{P0}\left[1 + \frac{X_W d_P}{d_W(1 - X_W)}\right] \tag{9a}$$

$$V_{\beta-G}(a_W) = V_{\beta-G0}\left[1 + \frac{X_W d_{\beta-G}}{d_W(1 - X_W)}\right] \tag{9b}$$

$$V_{CW}(a_W) = V_P(a_W) + V_{\beta-G}(a_W) \tag{9c}$$

$$\phi_P(a_W) = \frac{V_P(a_W)}{V_{CW}(a_W)};\ \phi_{\beta-G}(a_W) = \frac{V_{\beta-G}(a_W)}{V_{CW}(a_W)} \tag{9d}$$

The isotherm of sorption of the composite structure is then calculated according to eq 6 and is the sum of the two isotherms of sorption affected by their volume fractions:

$$X_{WM} = \frac{X_{mP} K_P C_P a_W}{(1 - K_P a_W)(1 - K_P a_W + K_P C_P a_W)}\phi_P(a_W) + \frac{X_{m\beta-C} K_{\beta-C} C_{\beta-C} a_W}{(1 - K_{\beta-C} a_W)(1 - K_{\beta-C} a_W + K_{\beta-C} C_{\beta-C} a_W)}\phi_{\beta-C}(a_W) \tag{10}$$

In **Figure 10b** are represented the experimental data, the direct GAB fit, and the reconstruction of a composite behavior using eq 10. A good agreement is observed between these sets of data, which validate the bilayer model. If now we consider the inner radius (r_{inner}) of the cell wall as independent of the water uptake

and a homogeneous external surface, the surface (S) of the cell can be estimated for any water activity using:

$$S(a_W) = 4\pi\left[\frac{3V_{CW}(a_W) + 4\pi r_{inner}^{3}}{4\pi}\right]^{2/3} \quad (11)$$

Figure 10c shows the relative surface increase due to the swelling of the cell wall.

The surface increase in this ultimate case (homogeneous surface) shows a maximum of around 33% increase as compared to the surface of the dry cell. The fitting GAB parameters of the bilayer calculation are for X_m, K, and C, 4.71 (experimental, 4.54), 0.860 (experimental, 0.872), and 3.62 (experimental, 3.29), respectively. These are close to the values obtained by fitting the experimental data at 20 °C (see **Table 1** or values in parentheses). This calculation demonstrates that both K and C GAB parameters can be approximated from the combination of the contribution of each layer affected by its solid weight fraction. However, the X_m value cannot be estimated from combining individual layers. Therefore, the GAB model in our case is only empirical and cannot be discussed further.

Visualization of the External Surface of the Yeast. In living cells, Kidby and Davies in 1970 (*24*) showed images of tears on the external cell wall of yeasts. In this work, the effect of water on the external cell wall structure has been imaged using AFM (**Figure 11a**,**b**).

In **Figure 11a**, 1 μm^2 of the surface of the yeast is scanned. The image shows a regular flat structure on which zones of different elasticity (light color = low elasticity and dark color = high elasticity) are coexisting. However, when the surface is wet, its structure is fully modified due to swelling (see **Figure 11b**). Some irregularities are observed on the surface as deep as 200 nm, and layers of different elasticity are superposed (the lighter sits on the top of the darker). We interpret the image as an uncontrolled swelling of the external structure resulting in a breakdown of the cell's protection that creates spaces for exchanges with external medium (i.e., air, water, ...).

The increase in yeast surface looks higher than when calculated for uniform swelling, and the presence of pores on the surface is not clearly demonstrated. The cell wall does not swell uniformly in the presence of water keeping the release mechanism argument still open.

Limonene-Loaded Yeast Cells. *Effect of Flavor on Sorption Properties.* To see if the presence of the volatile inside the cells affects the water uptake, a simple mass balance analysis allows comparison of the water content on original yeast material. To do this, the mass of limonene should be excluded from the calculation. For both flavored and unflavored cells, we compare the quantity below:

$$X_W = 100\frac{m_{tot}(t) - m_s - m_F(t)}{m_{tot}(t) - m_F(t)} \quad (12)$$

Here, $m_{tot}(t)$ is the total mass of the sample, m_s is the mass of dry unflavored cells, and $m_F(t)$ is the mass of flavor that is not interacting with water. Therefore, the upper part in eq 12 is the mass of water and the lower part in eq 12 is the mass of the wet unflavored sample. The evolution of the mass of flavor with time is determined according to the rate of loss at each RH step. A good agreement is obtained between the water weight fraction of unflavored yeasts and flavored yeasts (using eq 12) when data shown in **Figure 7** are corrected by the loss of limonene as shown in **Figure 12** considering a perfect mass balance where only the limonene is evaporating and only the water condenses. This proves that the presence of limonene does not affect the hygroscopic behavior of the yeast.

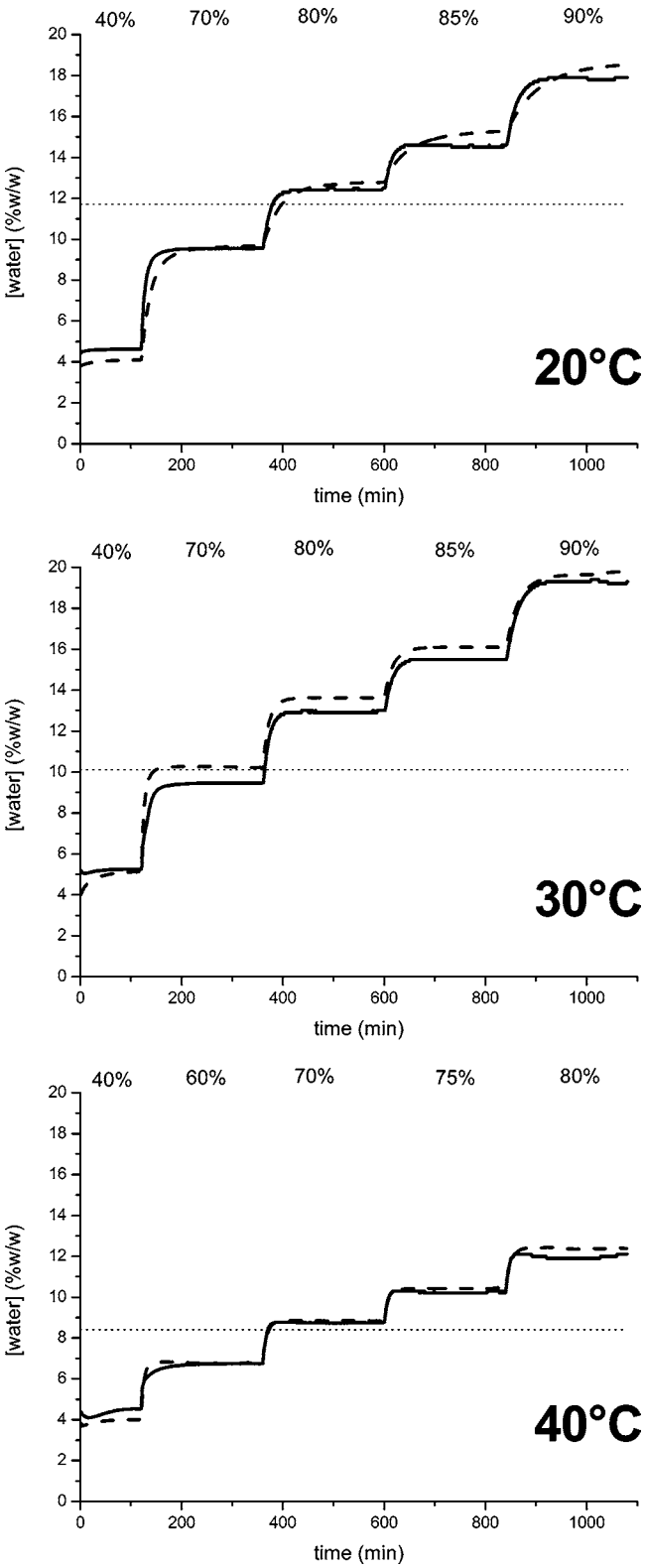

Figure 12. Concordance for corrected water uptake when the limonene loss is taken into account as if the flavored cells did not contain limonene (response of the shell) for three experimental temperatures. The lines correspond to the critical water content for the deformation of the cells.

Application to the Flavor Release Mechanism. Looking now at the release properties, two phenomena can be described using zero-order kinetics: either evaporation through holes when a pure liquid volatile is in an open environment (see eq 13a) or

diffusion through a membrane when the concentration of the liquid phase is constant (the concentration gradient through the membrane is constant) (see eq 13b). In both cases, the differential equation that describes the system follows:

$$-\frac{dm}{dt} = kSP_{vap} \quad (13a)$$

$$-\frac{dm}{dt} = DS\frac{dc}{dr} \quad (13b)$$

In eq 13a, m is the total mass of the volatile compound in the liquid phase, t is the time, k is the kinetic constant for the transfer of molecules from the liquid phase to the gas phase, S is the surface available for the exchange, and P_{vap} is the vapor pressure of the volatile at the considered temperature. In eq 13b, D is the diffusion coefficient through the membrane and dc/dr is the concentration gradient through the membrane of thickness (r). Equation 13a,b describes the same phenomenon; volatile molecules are transferred through the cell wall and reach the external surface of the yeast. If the limiting transfer is the evaporation from the surface to the gas phase, eq 13a applies whereas if the limiting transfer is the diffusion through a dense material, eq 13b applies. The solution of eq 13a,b is rather simple if the quantity dc/dr does not change with time (i.e., the volatile concentration on one side of the membrane is constant):

$$m(t) = m_0 - kSP_{vap}\,t \quad (14a)$$

$$m(t) = m_0 - DS\frac{dc}{dr}\,t \quad (14b)$$

Here, m_0 is the initial mass of the liquid sample. In the case of evaporation of a pure compound (eq 14a), k is independent of the RH. This is the partial vapor pressure of the volatile compound that drives the evaporation. Only the surface can affect the evaporation rate. If diffusion through the external shell is considered (eq 14b), the surface of exchange increases slightly due to the water uptake (toward a maximum value of 33% according to the model exposed earlier). However, more importantly, as water penetrates the yeast, the external cell wall swells. In this case, D increases when the mesh size of the shell increases. Therefore, the swollen composite network becomes more permeable to volatile molecules than when the network is dry.

As a conclusion, the evaporation of a pure compound in open conditions leads to a linear decrease of the total mass, as observed for yeasts containing limonene (see **Figure 7**). A more comprehensive study of the evolution of the rate of mass loss as a function of interactions between a volatile molecule and a polymer demonstrates that as soon as interactions exist, the rate of mass loss cannot be constant (*25*). Therefore, it is suggested that: (i) the material forming the membrane is not interacting with the volatile molecules, and the limonene is in contact with the air phase as if it was a simple, single liquid phase (presence of holes in the yeast cell wall); and (ii) the concentration gradient in the yeast cell wall (Fick's second law for diffusion eq 13b) is constant due to the presence of a reservoir containing 100% w/w of volatile at the inner side of the wall.

Through further evaluation of eq 14a (simple evaporation through holes in the membrane), the slope of the mass against time contains three parameters. The kinetic constant depends only on the temperature. The vapor pressure is a characteristic of the volatile and is well-defined. Therefore, the product $k \cdot P_{vap}$ is constant for a given temperature and independent of the water uptake. However, the slope of eq 14a is directly proportional to the surface of exchange.

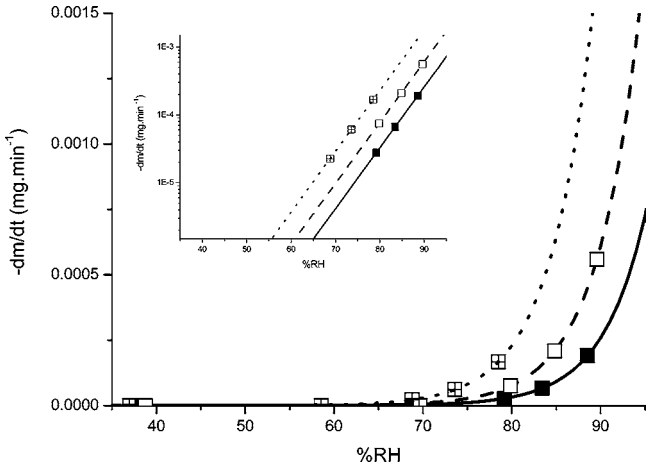

Figure 13. Evolution of the rate of evaporation of limonene at 20 (solid line), 30 (dashed line), and 40 °C (dotted line) as a function of the RH. The best fits are exponential.

If Fick's second law for diffusion is considered (eq 14b), it has exactly the same format than eq 14a if the kinetics constant is replaced by the diffusion coefficient and the vapor pressure (that is constant in eq 14a) is replaced by the concentration gradient (that is also constant in the case of a constant concentration on one side of the membrane). However, the diffusion through the cell wall is now dependent on the mesh size of the polymeric network that forms the cell wall and D should increase as the concentration of polymer decreases (*20*). The quantity $D \cdot S$ becomes the only parameter that controls the kinetics of release as the cell wall swells.

In this article, we discuss the evolution of the surface of exchange considering both cases, namely, evaporation through holes or diffusion through cell walls. The experiments conducted here are made in isothermal conditions. Therefore, on one hand, one can consider $k \cdot P_{vap}$ constant, and on the other, dc/dr is constant and independent of the RH. Thus, the modification of release is either due to the surface modifications or due to the surface and diffusion coefficient increase.

By increasing the RH in air, the slope of the mass vs time becomes steeper (**Figure 13**). This is in favor of an increase in the surface of exchange, either pore size or pore number, that open locally the membrane or swelling of the whole surface of the yeast.

At 70% RH, when the rate of evaporation becomes measurable, a water mass fraction of around 9% w/w is determined (GAB model). Similarly, at 20 and 30 °C, the release slope becomes significantly measurable for RH over 70%. It is then interesting to consider the 70% RH as well as the limit of humidity conditions for which yeasts multiply.

The rate of mass loss is only due to the evaporation of limonene: When water (% RH) is added to unflavored yeasts, the mass is stable. However, the rate of loss of volatile increases exponentially with the RH between 20 and 40 °C and a very good fit can be drawn ($R^2 = 1$) (see **Figure 13**). An exponential fit of these data demonstrates that limonene evaporates from loaded yeast cells whatever the RH conditions. This explains the headspace over the dry loaded yeasts powder (*26*). However, the rate becomes significant at 80% RH, which means that the stability of this encapsulation technology is quite high.

The rate of limonene loss can be expressed empirically as a function of both the RH between 40 and 90% and the temperature between 20 and 40 °C:

$$\ln\left(-\frac{dm_L}{dt}\right) = a \cdot RH + \ln(b_0) + \frac{1000c}{T} \qquad (15)$$

where m_L is the mass of limonene, t is the time (min), RH is the RH, T is the temperature (K), and a, b_0, and c are the three fitting parameters. The best fit under these conditions is obtained for $a = 0.206$, $b_0 = 33.33$, and $c = -8.91$ K. The values of the three parameters describing the evolution of the evaporation rate as a function of the temperature and the RH are strongly dependent on the vapor pressure of the substance to evaporate. The figure given here concerns only limonene but allows a good understanding of the release mechanism in the present case.

Let us assume that the collapse temperature is one indicator for the release to start as suggested earlier. We have demonstrated previously that the mechanical properties of the external shell are affected by the presence of water. A quick modeling to estimate the collapse temperature corresponding to a given quantity of water content is necessary to illustrate our theory.

Modeling Collapse Temperature. The collapse temperature is successfully fitted by an empirical nonlinear regression that is analogous to the Gordon Taylor equation used for Tg (*27*). This is preferred to the simple linear regression as it can be assimilated to a similar change in material properties.

$$T_c = \frac{\omega T_0 + k(1-\omega)T_\infty}{\omega + k(1-\omega)} \qquad (16)$$

In eq 16, ω is the water mass fraction, T_0 and T_∞ are the collapse temperatures for zero yeast content and for zero water content, respectively, and k is the parameter for the curvature. A satisfactory fit is obtained for T_0 and T_∞ equal to -134 and 115 °C, respectively, and k equals to 4.53. When measurements are performed in isothermal conditions, this model allows determination of the water content necessary for the sample to collapse. The construction is shown in **Figure 14a**. Also, according to the GAB model (see **Figure 10b**), it becomes possible to estimate the RH condition for the considered temperature necessary to reach the critical water content. This is shown in **Figure 14b** for the three temperatures investigated. Once the critical water activity is known, the rate of loss is determined according to eq 15 as shown in **Figure 14c**. The critical water content and the critical RH are resumed in **Table 2** for the temperatures investigated.

Using eq 15, it is possible to calculate the initial rate of loss at the critical RH for the three temperatures. All of the rates of limonene evaporation are quasi-identical at this critical point ($-dm/dt = 1.43\ 10^{-5} \pm 0.13\ 10^{-5}$ mg min^{-1}), which is an indication that the physical structure of the shell is the key to release. Also, one can conclude that before the critical point, the structure is hard to deform and closed; therefore, no release is permitted, and at the critical point, the structure becomes deformable but also allows evaporation, which is an indication of an open structure.

A characterization of the flavor release mechanism from yeast loaded with hydrophobic volatile flavor compounds (in this case limonene) is presented. This mechanism is based on precise microscopic observation together with physical properties of the yeast either loaded or empty. The flavor that is localized inside the phospholipid bilayer can be released according to two identified ways: thermal treatment, when the temperature exceeds 260 °C, or action of water on the structure of the yeast cell wall, when the water activity exceeds 0.7. Therefore, two descriptive mechanisms of limonene release from loaded yeasts are elucidated and discussed. The first mechanism, related to temperature stress, demonstrates that loaded yeast retains flavor at temperatures higher than those applied in most of the food processes and makes yeast cells a very heat stable flavor encapsulation system. The second mechanism, related to water activity, depends on the cell wall structure/properties relationships, especially water sorption and desorption. An on/off release mechanism is described that depends on RH or water activity. This is a very unusual mechanism that has never been observed in most conventional encapsulation systems.

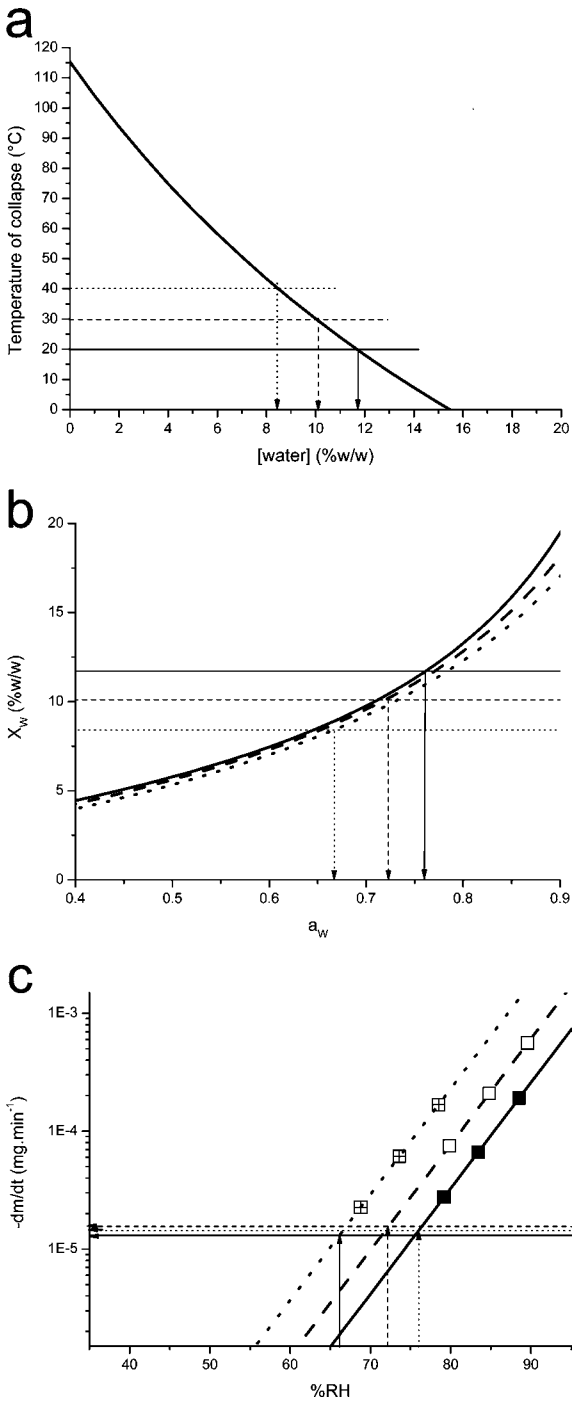

Figure 14. (**a**) Determination of the critical water content at the apparent transition for 20, 30, and 40 °C. (**b**) Determination of the water activity in equilibrium with the solid sample to reach the critical water content determined using the same construction as in **Figure 10a** at 20, 30, and 40 °C. (**c**) Determination of the rate of flavor evaporation at the critical water content.

Table 2. Critical Quantities and Rate of Mass Loss at the Apparent Transition

temp (°C)	X_W critical (% w/w)	a_W critical	$-dm/dt$ (mg min^{-1})
20	11.7	76	$1.30\ 10^{-5}$
30	10.1	72	$1.56\ 10^{-5}$
40	8.4	67	$1.43\ 10^{-5}$

Thermarome is a new Firmenich encapsulation carrier that involves encapsulation of active flavor molecules in yeast. Those two release mechanisms are the keys for the exceptional performance of this delivery system. For example, in French fries, it can resist the high temperature of the frying process and release the flavor when hydration occurs in the mouth.

ACKNOWLEDGMENT

Dr. L. Ouali and D. Benczédi are greatly acknowledged for technical support and useful discussions and D. Ferdinando and D. Atkins from Unilever Research Colworth for producing the electron microscopy. Dedicated to Dr F. Naef on the occasion of his 65th birthday.

LITERATURE CITED

(1) Bishop, J. R. P.; Nelson, G.; Lamb, J. Microencapsulation in yeast cells. *J. Microencapsulation* **1998**, *15* (6), 761−773.
(2) Pannell, N. A. Microbial encapsulation. European Patent 0 242 135, 1990.
(3) Sagar, B. F.; Sagar, A. J. G.; Graham, S. G.; Wragg, R. T. Method for encapsulating substances in biocapsules. U.S. Patent 5,660,769, 1997.
(4) De Nobel, J. G.; Klis, F. M.; Munnik, T.; Priem, J.; Van Den Ende, H. An assay of relative cell wall porostity in *Saccharomyces cerevisiae*, kluyveromyces lactis and schizosaccharomyces pombe. *Yeast* **1990**, *6*, 483−490.
(5) Nelson, G.; Crothers, M. E. D. Microencapsulation in yeast cells and application in drug delivery. *Polym. Mater.: Sci. Eng.* **2003**, *89*, 146.
(6) Inoue, C.; Ishiguro, M.; Ishiwaki, N.; Yamada, K. Process for preparation of microcapsules. European Patent, 0 453 316 B1, 1991.
(7) German, R. J.; Morris, G. G.; Pannell, N. A. Process for encapsulating substances by means of microorganisms, and the encapsulated products obtained thereby. European Patent, 0 085 805B1, 1982.
(8) Cabib, E.; Roberts, R.; Bowers, B. Synthesis of the yeast cell wall and its regulation. *Annu. Rev. Biochem.* **1982**, *51*, 763−793.
(9) McLellan, W. L.; McDaniel, L. E.; Lampen, J. O. Purification of phosphomannanase and its action on the yeast cell wall. *J. Bacteriol.* **1970**, *102*, 261−270.
(10) Brunauer, S.; Emmett, P. H.; Teller, E. Adsorption of gases in multimolecular layers. *J. Am. Chem. Soc.* **1938**, *60*, 309−319.
(11) Zlotnick, H.; Fernandez, M. P.; Bowers, B.; Cabib, E. *Saccharomyces cerevisiae* mannoproteins form an external cell wall layer that determines wall porosity. *J. Bacteriol.* **1984**, *159* (3), 1018−1026.
(12) Anderson, R. B. Modifications of the Brunauer, Emmett and Teller Equation. *J. Am. Chem. Soc.* **1946**, *68*, 686−691.
(13) Radosta, S.; Schierbaum, F.; Reuther, F.; Anger, H. Polymer−water interaction of maltodextrins, Part 1: Water vapour sorption and desorption of maltodextrin powders. *Starch/Stärke* **1989**, *41* (10), 395−401.
(14) Scherrer, R.; Louden, L.; Gergardt, P. Porosity of the yeast cell wall and membrane. *J. Bacteriol.* **1974**, *May*, 534−540.
(15) De Nobel, J. G.; Dijkers, C.; Hooijberg, E.; Klis, F. M. Increased cell wall porosity in *Saccharomyces cerevisiae* after treatment with dithiothreitol or EDTA. *J. Gen. Microbiol.* **1989**, *135*, 2077−2084.
(16) Avaltroni, F.; Bouquerand, P.-E.; Normand, V. Maltodextrin molecular weight distribution influence on the glass transition temperature and viscosity in aqueous solutions. *Carbohydr. Polym.* **2004**, *58* (3), 323−334.
(17) Slade, L.; Levine, H. Beyond water activity: Recent advances based on an alternative approach to the assessment of food quality and safety. *Crit. Rev. Food Sci. Nutr.* **1991**, *30* (2−3), 115−360.
(18) Timmermann, E. O. Multilayer sorption parameters: BET or GAB values? *Colloids Surf., A* **2003**, *220*, 235−260.
(19) Teng, C. D.; Zarrintan, M. H.; Groves, M. J. Water vapor adsorption and desorption isotherms of biologically active proteins. *Pharm. Res.* **1991**, *8* (2), 191−195.
(20) Bouquerand, P. E.; Maio, S.; Normand, V.; Singleton, S.; Atkins, D. Swelling and erosion affecting flavor release from glassy particles in water. *AIChE J.* **2004**, *50* (12), 3257−3270.
(21) Gomi, Y. I.; Fukuoka, M.; Mihori, T.; Watanabe, H. The rate of starch gelatinization as observed by PFG-NMR measurement of water diffusivity in rice starch/water mixtures. *J. Food Eng.* **1998**, *36*, 359−369.
(22) Strumillo, C.; Kuts, P. S.; Akulich, P. V.; Kaminski, W. Hygroscopic properties of biological materials and the binding energy of moisture. *J. Eng. Phys. Thermophys.* **1994**, *67*, 1093−1097.
(23) Weisser, H. *Properties of Water in Foods*; Simatos, D., Multon, J. L., Eds.; Martinus Nijhoff: Dordrecht; p 95.
(24) Kidby, D. K.; Davies, R. Invertase and disulphide bridges in the yeast wall. *J. Gen. Microbiol.* **1970**, *6x*, 327−333.
(25) Ouali, L.; Léon, G.; Normand, V.; Benczédi, D. Mechanism of Romascone release from hydrolyzed vinyl acetate particles: A thermogravimetric method. *Polym. Adv. Technol.* Submitted for publication.
(26) Nicolas, L.; Baumgartner, P.; Steenhoudt, M.; Normand, V. Thermarome a yeast based delivery system from Firmenich with optimized flavor release. *Chin. Food Ind. J.* Submitted for publication.
(27) Gordon, M.; Taylor, J. S. Ideal copolymers and the second-order transitions of synthetic rubbers. I. Noncrystalline copolymers. *J. Appl. Chem.* **1952**, *2*, 493−500.

Received for review April 7, 2005. Revised manuscript received July 6, 2005. Accepted July 10, 2005.

JF0507893